Artificial Intelligence-Controlled Photovoltaic Generator for Optimized Power Point Tracking

Cristian Orellana[1], *Viviana* Moya[1,*], *Marcelo* Moya[1], and *Cristina* Oscullo[1]

[1]Facultad de Ciencias Técnicas, Universidad Internacional Del Ecuador UIDE, Quito 170411, Ecuador

Abstract. This paper addresses the pressing need for sustainable energy solutions by focusing on developing a photovoltaic solar tracker enhanced with artificial intelligence (AI). The current and future global trends challenge energy systems to improve their output while also maintaining an eco-friendly approach, and there is an option to offset carbon emissions through photovoltaic energy. Nevertheless, the solar panel's efficiency depends upon its ability to follow the sun's movement to find the optimum energy angle. This project offers a unique solution, adopting a neural network technique that was trained using weather data from the daily weather forecasts to determine the correct angles of the panel at all times. The sampling unit was fabricated using aluminium and PLA materials and monitoring parameters of temperature, humidity, radiation, pressure, and atmospheric variables. A web-based interface lets monitor the system in oh-so-real-time and delivers graphical presentations of crucial metrics, including voltage, current, and power production. The outcomes suggest a significant enhancement in energy output, which ascends from 22.65% to 29.25%, equivalent to a 144.56 kWh-year rise. Although the margins of profitability may differ by region, our study sheds light on the efficiency of this AI-integrated solar tracker, especially in regions like Brazil or Spain, which facilitates alternative energy policies with possible economic benefits.

1 Introduction

The National Electric Energy Balance of Ecuador in 2023 reveals that the primary sources of electrical energy generation in the country are: hydroelectricity (62.46%), photovoltaic energy (0.34%), wind energy (0.86%), biomass (1.35%), and biogas (0.09%). The remaining 34.60% is derived from non-renewable fossil fuel sources. This is further divided into 19.78% from internal combustion engines, 9.59% from turbo gas, and 5.23% from turbo steam [1]. The institution responsible for efficiently facilitating transactions of electrical products between generators and consumers is the "Operador Nacional de Electricidad - CENACE". Nevertheless, the need for electricity in Ecuador continues to increase every year, necessitating the exploration of various ways of generation in energy planning. One of the strategies is the establishment of solar-powered facilities. The corporation currently has a power-producing facility for its own use. However, the solar panels they utilize remain stationary and fail to fully harness the potential energy they may accumulate over the day. Considering this, it becomes interesting to develop an automated maximum power point tracking system that may enhance the electrical energy generation of a photovoltaic panel.

*Corresponding author: vimoyago@uide.edu.ec

The International Energy Agency (IEA) reported that a remarkable 81% of the global primary energy supply was sourced from fossil fuels as of 2019 [2]. Europe, in this context, takes the lead in reducing reliance on fossil fuels, with countries like Denmark and Germany establishing high standards through ambitious policies and projects. Denmark's impressive incorporation of wind energy at a rate of 45% and Germany's effort, which has resulted in a renewable mix of 38%, demonstrate the region's dedication to sustainable energy solutions. On the other hand, Asia, namely China and India, is experiencing a significant surge in the adoption of renewable energy. This is mostly due to the massive expansion of the solar and wind industries. The yearly development rate of 30% in these sectors in China and India's intention to achieve a 40% renewable capacity by 2030 demonstrates their dedication to integrating industrial advancement with sustainability objectives [3].

The American continent exhibits diverse levels of advancement, with the United States and Canada seeing significant development in the adoption of renewable energy, particularly through the utilization of wind, solar, and hydroelectric resources. The United States has successfully attained a renewable energy penetration rate of 27%, while Canada proudly claims a renewable energy mix of 29%. Brazil's substantial utilization of bioenergy plays a crucial role in its renewable energy portfolio, accounting for 33% of its total. Nevertheless, the African continent encounters obstacles because of its limited infrastructure and financial resources, despite its considerable solar capacity. The Middle East, which heavily depends on oil, is starting to expand its energy sources, with the United Arab Emirates (UAE) reaching a renewable capacity of 10% [4].

Prior studies have suggested various estimates for the global energy needs required to meet basic human needs in the future, taking into account advancements in technology and potential reductions in energy demand through behavioural changes. These estimates include 15.3 Giga Joules (GJ) per capita by 2050, 26.1 GJ per capita by 2050, or 42.4 GJ per capita by 2040. The per capita figures for 2050 are derived from the estimated global energy use of 245 Exa Joules (EJ) in Grubler's study, assuming a global population of 9.7 billion. Similarly, the figures for 2040 are based on an estimate of 390 EJ of total global energy use from the International Energy Agency (IEA), with a global population of 9.2 billion [5].

The global imperative to regulate conventional energy usage promotes the adoption of novel and environmentally sustainable energy generation options. To prevent the exploitation of non-renewable natural resources, which leads to atmospheric pollution, ecosystem imbalance, and a rise in the greenhouse effect, this approach could be adopted. As a result, renewable energy sources have made significant advancements in recent decades, establishing themselves as the primary energy source in the global market. These sources are very eco-friendly, sustainable, and cost-effective, with solar energy being one of the most efficient technologies in terms of energy usage [6].

Solar power is available worldwide, sustainable, cost-effective, and is a limitless energy source, and Ecuador is lucky to have significant solar potential. Ecuador, located in the equatorial zone, can consistently receive abundant solar radiation in specific areas of its land, enabling it to get up to 30% more solar radiation compared to other nations [7]. To fully harness the sun's potential as a renewable energy source, photovoltaic panels must receive the sun's rays at a perpendicular angle. Therefore, it is necessary to optimize the capture of irradiance using a solar tracking system. The tracking problem can be theoretically resolved by utilizing solar equations. However, in practical application, certain uncertainties are typically not considered, such as radiation or the prevailing environmental conditions [8]. The work of Zhikun (2016), consists of a system of a two-axis solar tracker, which includes a photoelectric sensor circuit, a GPS, and a current and voltage detecting circuit. In this instance, the astronomical algorithm was utilized to ascertain the azimuth and elevation angles to determine the sun's position. In addition, the perturb and observe method is being employed to monitor

the highest power point red[9]. Various sun-tracking techniques are currently employed in different nations, with variations arising due to differences in geographical conditions. The solar tracking technology that works in sectors close to the equator cannot be applied in the hemispheres. The next section will describe several projects that utilize trackers to address the same problem, showcasing the diverse range of solutions employed red[10].

The development of a two-axis tracking system is presented in the work of Reyes (2021). The tilt of this system is a function of the voltage, current, temperature, and radiation data it collects. The joints of the system move with the help of two NEMA motors. The project was developed in the city of Manta [11]. In the work presented by Fiallos (2020), they proposed a mathematical model based on Liu and Jordan's work to optimize the maximum power point of photovoltaic generation. This model enables examining the quantity of incident irradiance on a sloping surface [12]. The impact of dirt on the panel, as a variable with diffuse characteristics, is examined. The parameters allow the results to be shown from three different points of view: the data gathered by the meters, the inclination and orientation found using a compass and an inclinometer, and the result that was calculated based on the current conditions of the site. The article presented by Arpi (2022) explains the design of a two-axis solar tracker. This tracker utilizes irradiance and brightness sensors to determine the most favourable position for the panel. The microcontroller gathers data from the sensors by detecting variations in light levels throughout the day and uses this information to determine the optimal positioning of the panels. Geared motors are responsible for controlling each axis [13].

The paper by Mustafa (2018) describes a dual-axis tracker that utilizes light-dependent resistors (LDRs) to determine the sun's position precisely. The tracker utilizes an algorithm that processes the resistance values obtained from the sensors and generates the azimuth and elevation angles that accurately represent the sun's position. The tracker was created in the city of Baghdad [14]. Singh (2016) introduces a solar tracker that operates along a single axis and utilizes a parabolic-shaped reflector dish to maximize the capture of sunlight. The sun tracking method was implemented in Arduino, enabling the panel to rotate by 6.25 degrees every 30 minutes. The dish functioned analogously to a parabolic antenna, focusing all the waves at a single point and projecting them toward the panel [15].

A different approach is presented in the work of Mejia (2021) , where the discussion concerns a solar tracker that uses a fuzzy logic algorithm to identify the sun on two axes accurately. The system initially gathers the input radiation signals, then processes them, then applies fuzzy control, and ultimately adjusts the panel's rotation based on the algorithm's obtained result. The solar tracker has four radiation sensors assessed individually to ascertain the direction the panel should revolve. This approach incorporates fuzzy logic [16].

The solar tracker developed by Alarcón (2020) uses the perturb-and-observe technique to track the maximum power point accurately. This involves adjusting the duty cycle of the power converter connected to the solar panel's output, which changes the amount of current taken from the panel and affects the power output. Whenever there is a change in the measured power, the voltage is adjusted to restore balance in the system. This method is repeated until the maximum power point is achieved [17].

The ant colony algorithm presented by Sahoo (2017) optimised the maximum power point tracking. In situations where the panel receives varying amounts of irradiance throughout the day, the goal of this approach is to achieve optimal performance. The objective of ant colony optimization is to achieve a global maximum that would enhance the panel's efficiency [18].

According to Haider (2021), solar power is a sustainable energy source that can be transformed into electricity by harnessing sunlight at a right angle to the sun's beams. Nevertheless, stationary solar panels face difficulty producing sufficient energy due to their immovable positioning. A proposed prototype model for a solar tracking system with three-axis freedom

can track sunlight in various orientations. By aligning solar panels with the sun and tracking their trajectory throughout the day, this technique can enhance efficiency by 25% [19].

In the work presented by Agila (2021), the approach undertaken to construct a two-degree-of-freedom solar tracker is demonstrated. This system utilizes Light Dependent Resistor (LDR) sensors and an accelerometer to precisely determine the panel's position at a specific time of the day. The concept incorporates the utilization of linear actuators and a geared motor for the joints. The project was created in the city of Quito [20].

In contrast to the previous papers, this research uses artificial intelligence to analyze and develop a photovoltaic tracker system that optimizes energy collection. A neural network is responsible for processing the data and providing the azimuth angle, elevation angle, and motor rotation angle, which are subsequently transmitted to the microcontroller. This technique is continued at five-minute intervals throughout the entire day. The artificial intelligence algorithm has undergone training using pertinent historical data from February 2007 to March 2022. The climatic characteristics considered for the neural network include temperature, humidity, air pressure, and radiation. The system aims to enhance the efficiency of photovoltaic energy generation by implementing a sun-tracking system. Additionally, it conducts a comprehensive review of the system's profitability over time.

This paper is structured as follows: Section 2 provides an overview of the mechanical, electronic and software designs, the materials used and the followed methodology. Section 4 shows the data and plots obtained during the tests performed with the prototype. Then, Section 4 provides a comparison of the performance of the proposed machine against other studies. Finally, Section 5 offers concluding remarks and insights from the research.

2 Materials and Methods

The proposed solar tracker is a prototype that combines mechanical, electronic, and computational components. A general machine scheme is presented in Fig 1. The composition can be divided into pivoting devices and the structure that conceals them. The electronic parts consist of a microcomputer board, various sensors, and actuators that power the turning wheels. The software part encompasses the algorithm used in the process, the developed artificial intelligence model, and the web interface that allows monitoring of the panel's performance.

2.1 Mechanical design

The mechanical section includes the solar panel, the structure that supports the panel and transmission mechanisms as indicated in Fig. 2.

The solar panel used is the Yingli Solar YL250P-29b (250W). Regarding the structure, firstly, a single-axis tracking system is defined, with a structure sized under load analysis, one side of the structure was analyzed considering as loads: the weight of the panel, the weight of the gearbox, the torque for rotation of the solar panel and the wind resistance is neglected due to the change in position is gradual, with this analysis and the availability on the market of aluminium profiles, the Bosch Rexroth AG 40×40 profiles are used.

To transmit the torque produced by the motor to the panel, it was decided to work with a single-gear worm mechanism, which is a one-way mechanism, considering the inconvenience of placing the motor shaft to the panel for reasons of protection of the motor against environmental conditions.

The gears were geometrically dimensioned and implemented with 3D printing techniques validated by stress analysis. The gear system has a 95 mm pinion @ 50 rpm and transmits 60

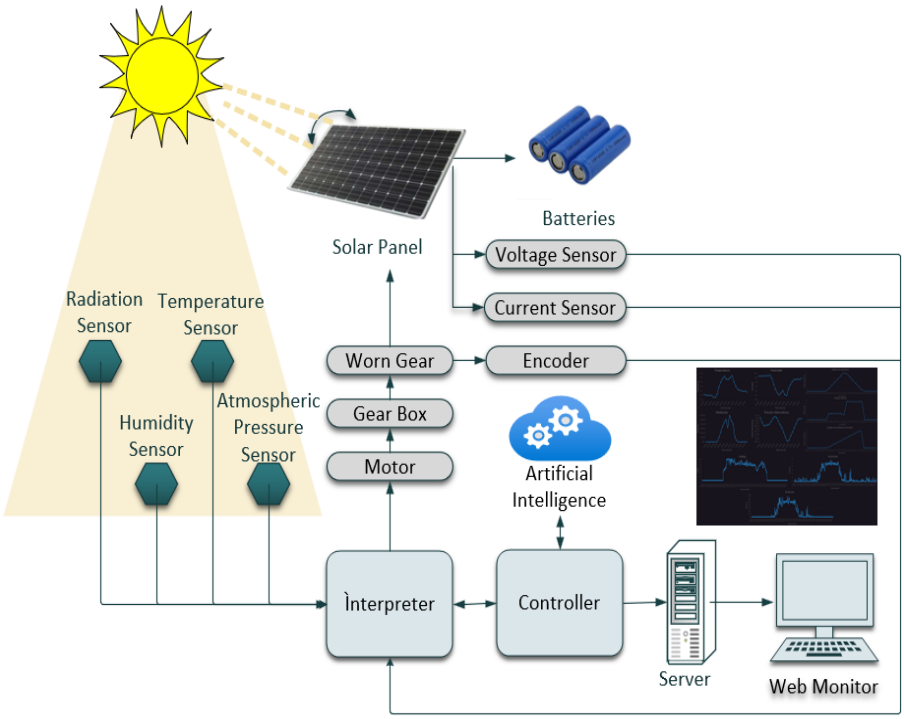

Figure 1. General Scheme of the Prototype.

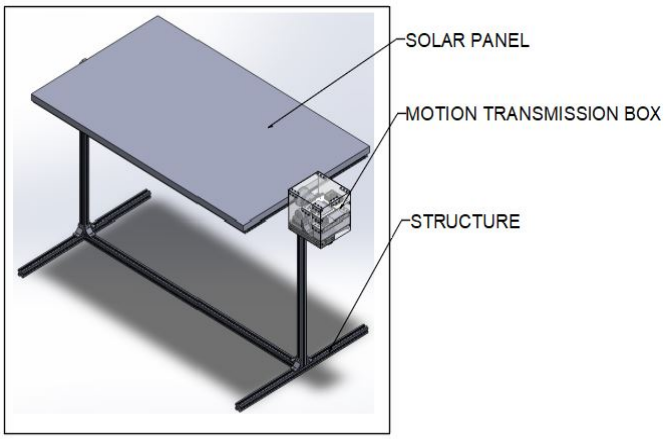

Figure 2. Mechanical scheme.

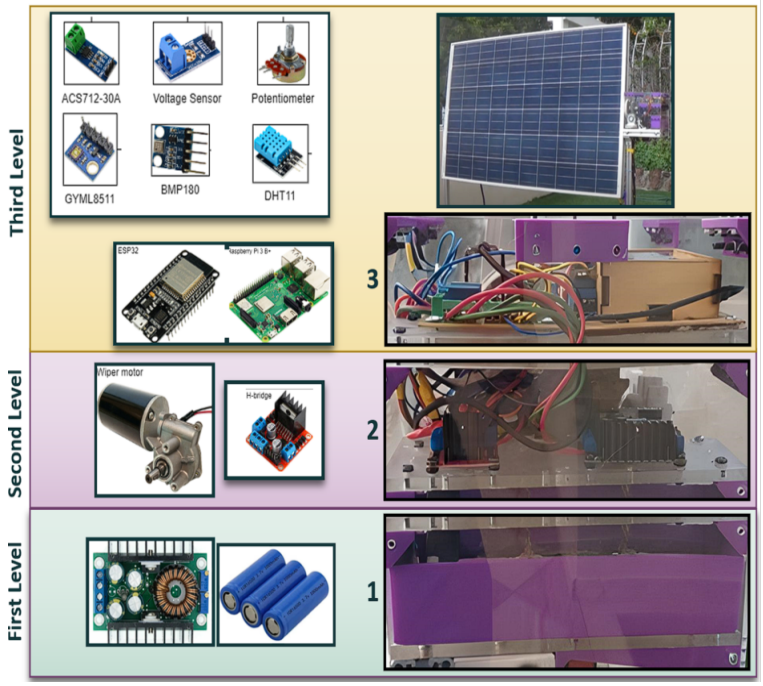

Figure 3. Electronic scheme.

W to the wheel, and the pressure angle between the two is 30º. The material used is PLA with an elastic limit of 55 MPA. Wheel, and that the pressure angle between both is 30º. The motion transmission includes a single-gear worm mechanism made of aluminium. This material was chosen because it is used for mechanized elements, and gear worm must be manufactured applying this technique. Additionally, due to their characteristics, this material will support all the stresses applied over the mechanism, and it is good for outdoor applications.

2.2 Electronic design

The electronic section of the project concerns selecting and deploying components that will allow the solar tracking system to perform at its maximum potential. The process will proceed as follows: First, various environmental sensors, motors, and batteries will be provided to ensure real-time working and to manage the movement of the photovoltaic panel. The next Fig. 3 shows all the electronic components used.

2.2.1 redComputer:

Due to its versatility and compact size, the system's control hub will be a Raspberry Pi 3 B+. Equipped with digital pins, it can interface with sensors and actuators, while its ability to execute Python scripts simplifies programming. Its small form factor allows seamless integration, and remote monitoring via VNC viewer eliminates the need for a dedicated display.

Table 1. List of sensors

Variable	Sensor	Voltage	Current	COM
Irradiance	GYML8511	2.7 V to 5.5 V	5 mA	ADC
Atmospheric pressure	BMP180	1.7 V to 3.6 V	5 μA	I2C
Humidity and Temp.	DHT11	1.8 V to 3.6 V	2.5 mA	Digital
Voltage	Voltage divider	3.3 V	NA	ADC
Current	ACS712-30A	5 V	NA	ADC
Angle	Potentiometer 20 kΩ	3.3 V	NA	ADC

2.2.2 redSensors:

A diverse array of sensors is essential for the system, measuring radiation, atmospheric pressure, humidity, and temperature. To collect data on solar panel generation, a voltage divider and current sensor are proposed. Additionally, detecting the panel's positioning necessitates implementing an encoder with a potentiometer. These sensors are listed in Table 1. However, a challenge arises with some sensors as their outputs are analog, incompatible with Raspberry Pi's reading ports. To address this, an intermediary solution enabling sensor reading is sought.

2.2.3 redComplementary device:

Addressing Raspberry Pi's limitations regarding analog pins necessitates the integration of external ADCs to convert analog signals into digital ones. However, these modules are relatively uncommon and have a hefty price tag. An alternative approach is to utilize another board equipped with internal ADCs capable of communicating with the Raspberry Pi via serial connection. The ESP32 was chosen. This low-power microcontroller boasts a dual-core ESP-WROOM-32 module supporting MCU functionalities along with dual-mode Wi-Fi and Bluetooth communication. The central controller offers flexibility with two power supply options: USB and an external 3.7V lithium battery [21].

2.2.4 redDC Voltage Regulator:

The XL4016 was chosen to regulate the solar panel's 25 V to 35 V output down to 12 V for the circuitry. This variable voltage buck converter efficiently reduces voltage with an input range of 8V to 40V and an output range of 1.25 V to 36 V, supporting up to 8 A current and 300 W power.

2.2.5 redBattery Management System and Battery Pack Array

The solar panel generates energy that needs to be stored in a battery. To charge the battery efficiently, we need a device that can handle it. That's where the XL4016 comes in. It can charge three Li-ion batteries in series, with a maximum tolerance of 25 A. The device operates within the 10.8 V to 13 V charge voltage range and with a charge voltage from 4.25 V to 4.35 V, ensuring optimal battery performance. The discharge voltage ranges from 2.3 V to 0.5 V.

The battery pack consists of 3×3 lithium-ion batteries, each 18-mm diameter and 65-mm length. These batteries are also known as Li-Ion batteries and are cylindrical. They are high-efficiency and high-quality batteries with a rated voltage of 3.7 V and a storage capacity of 2200 mAh. The nine batteries are connected in an array, providing a total storage capacity of 11.1 V, 6.6 Ah, and 73.26 Wh, making it an efficient energy storage solution for the system.

2.2.6 redMotor Controlling and DC Motor

To achieve the project's objective of rotating the solar panel from east to west and vice versa, a circuit capable of controlling the motor's direction is necessary. For this purpose, an H-Bridge is employed. This circuit can switch the polarity of the voltage applied to the load, facilitating control over the direction of rotation. Comprising two pairs of transistors, the H-Bridge opens or closes to manage the direction of the control current, determining the rotating direction. When selecting a motor, considerations include rotational speed and required torque. For this application, where the photovoltaic panel requires slow horizontal rotation, a maximum rotational speed of 5 rpm and a 50 N · m mechanical torque are assumed. A suitable option in the market is a 12 V, 50 rpm, 60 W DC wiper motor, effectively meeting the project's requirements.

2.3 Artificial Intelligence Algorithm

Selecting the optimal machine learning architecture for the project requires thoroughly analyzing the training data. First, ambient data such as temperature, radiation, humidity, and atmospheric pressure was obtained from the official website of the "Secretaría del Ambiente del Municipio del Distrito Metropolitano Quito" [22]. This dataset, spanning from February 2007 to March 2022 and comprising hourly measurements, consists of 132,407 rows, providing ample data for the application's needs.

Second, azimuth and elevation angles since 2007 were sourced from [23], which facilitates the determination of the sun's position worldwide, with data explicitly filtered for Ecuador. These angles also inform the calculation of the panel's current inclination m using (1), where e and a denote elevation and azimuth angles, respectively, and n represents the current array element.

$$m_n = \begin{cases} e_n & a_n \leq 200 \\ e_n - e_{n+1} + m_{n-1} & a_n > 200 \end{cases} \tag{1}$$

In Fig. 4, scatter plots depicting the relationship between two variables independent from others are presented. These graphs serve to assess the correlation between outputs and inputs. Despite considerable dispersion among data points, discernible linear and nonlinear relationships emerge, which are crucial for this project's analysis. This observation is corroborated by the heatmap depicted in Fig. 6, where nearly every output exhibits a correlation coefficient exceeding 0.5, indicating significant positive or negative relationships. The sole exception is the correlation between elevation and atmospheric pressure, registering at 0.17.

Following the preliminary analysis and considering the dataset comprising four inputs and three outputs, a multioutput neural network was developed for prediction. The proposed architecture entails an input layer with 4 neurons, 3 hidden layers with 100 neurons each, and an output layer with 3 neurons. This design achieves an accuracy of 0.88, 0.86, and 0.92 for the elevation, azimuth, and panel inclination angles, respectively. Fig. 6 shows a basic diagram of the implemented neural network, including inputs, outputs, and layers.

2.4 Web interface monitor

The view element consisted of three linked webpages: credential webpage, user management webpage and dashboard webpage. The first is the one that requires the person to enter their username and password. After, the management section, in which the person can select the actions that are available for him, depending on his permissions. One of those options is to monitor the panel, so that button must be selected, and he goes to the dashboard section.

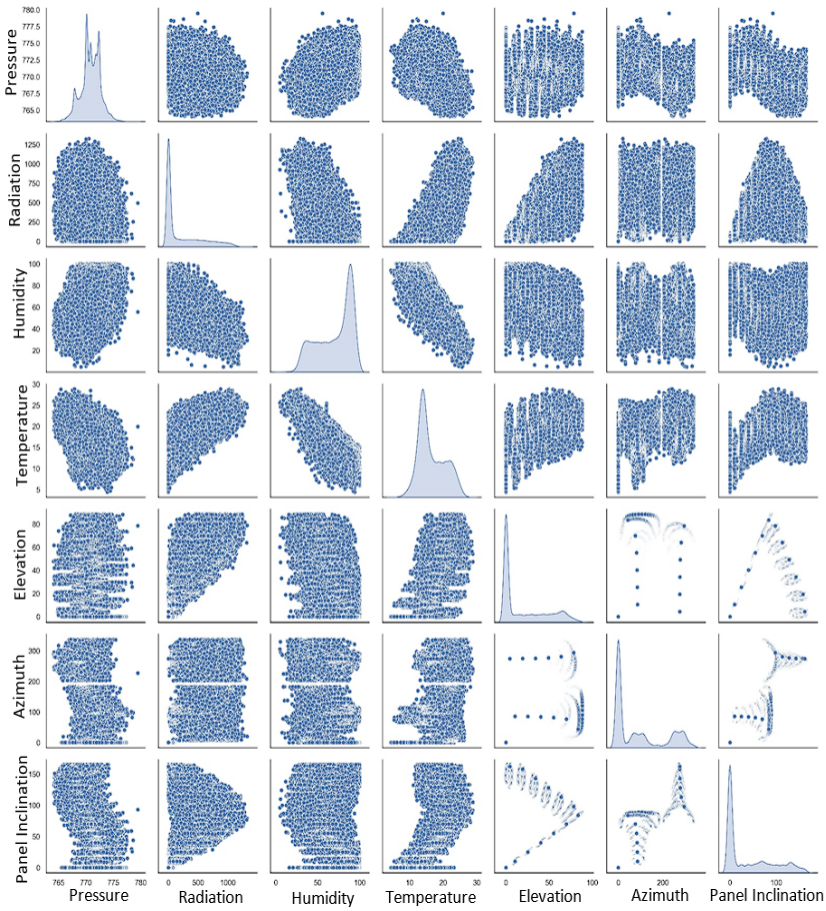

Figure 4. Scatter plots of the input and output data.

In this part, there is the option to select the day to review, and the corresponding weather, generation, and solar inclination graphs during the day appear below. Some examples of these graphs can be seen in Fig. 7, Fig 8 and Fig. 9.

3 Results

The way to determine if the performance of the prototype is the desired, considering this only is made up with one solar panel, is to measure the power production in two different days or months with similar ambient characteristics [24]. This is the best option for testing because the same panel is being used with the same conditions. If the test is realized with two different panels, the final information could be biased.

So, this project was tested by getting the power generation data from the static solar panel during one week (November 7th to November 13th of 2022) and from the rotating solar panel during the next week (November 14th to November 20th of 2022), in Nayón - Quito (latitude -0.161769 and longitude -78.446716). The mean generation from both was calculated to see the week's production. It is important to clarify that the solar panel was not completely horizontal during the first week due to the dust and rain; it was quite 15º tilted [12].

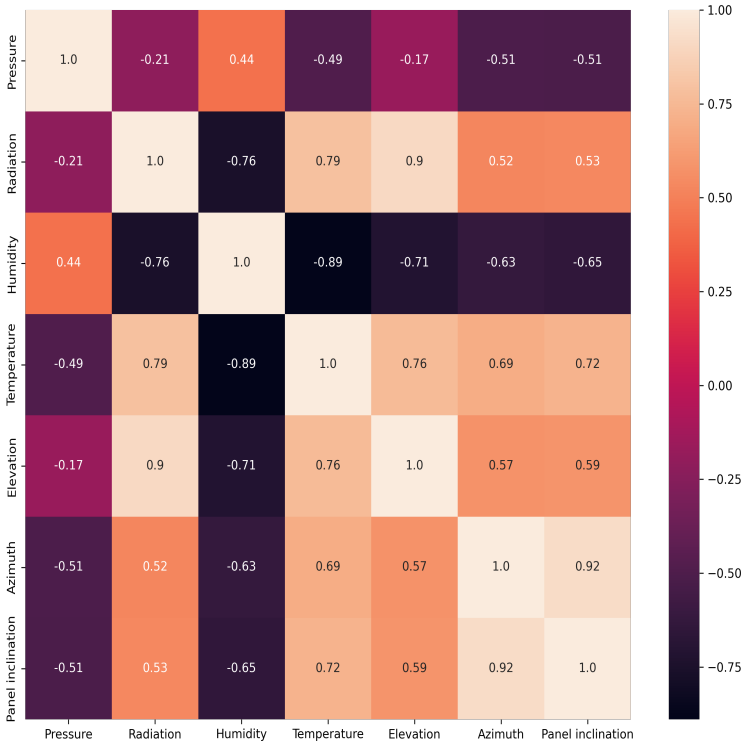

Figure 5. Heat map of the dataset.

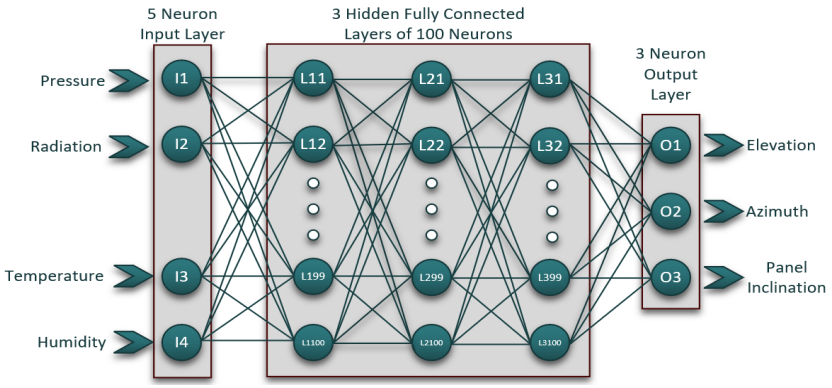

Figure 6. Basic Diagram of the Implemented Neural Network.

In Fig. 10, the orange line represents the generation without the tracking system, while the blue one represents the generation with it. As it can be seen, the peak value for the static position was at 10:00 because of the 15º tilting; for this reason, the orange line overwhelmed the blue at that hour. However, the rotating-system generation is greater than the other most of the time.

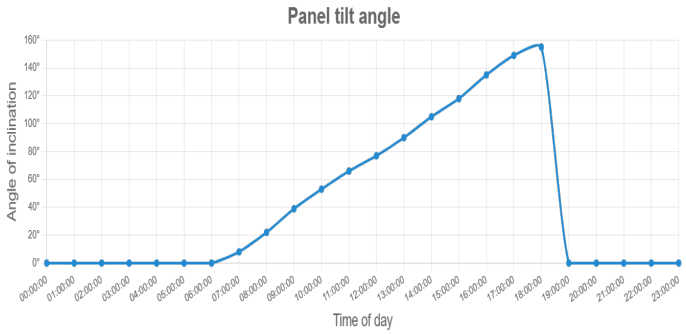

(a) Solar panel inclination angle

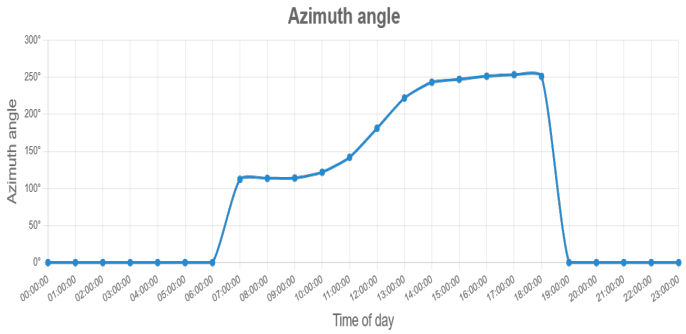

(b) Azimuth angle

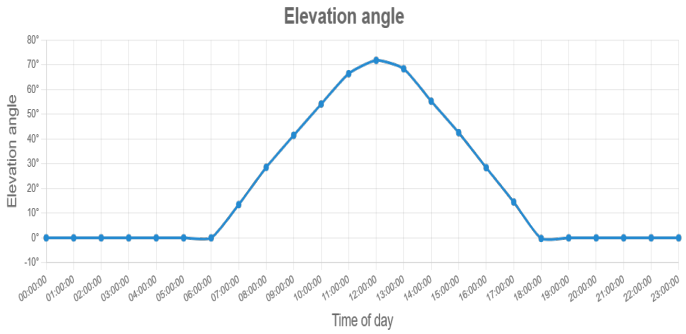

(c) Elevation angle

Figure 7. Examples of angle graphs shown in the webpage.

In a week, the static system generated 10214.82 Wh when the solar panel was static, while it generated 12994.85 Wh when it was rotating. This means that the total static production is estimated to be 531.17 kWh-year, while the rotating one would be 675.73 kWh-year.

Now, the total energy consumption was determined to verify if the prototype would be profitable, taking into account the consumption of all the devices mentioned in Section 2. This value is 4.02 Wh, which represents 96.52 Wh up to date. This implies 35.23 kWh-year is needed to run the prototype for one year.

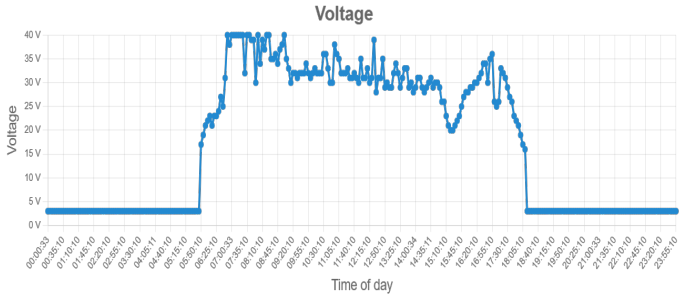

(a) Generated voltage

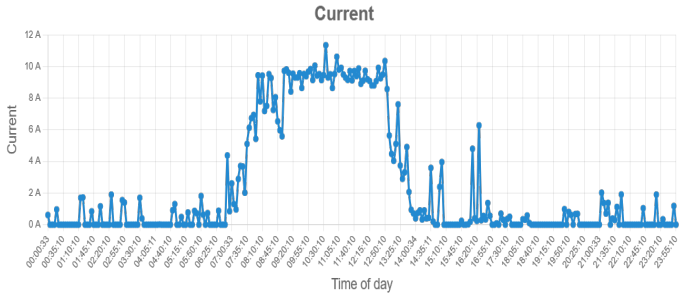

(b) Generated current

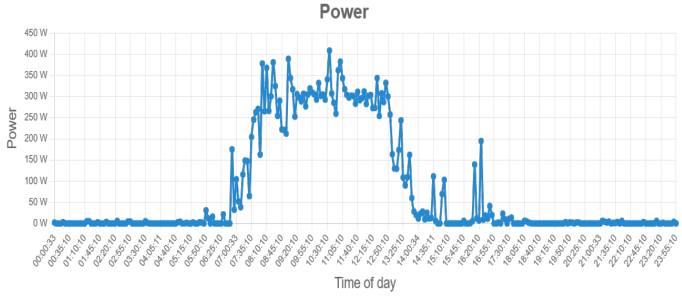

(c) Generated power

Figure 8. Examples of generation graphs shown in the webpage.

To get the final production, the consumption must be subtracted from each total. The system generated 495.94 kWh-year and 640.50 kWh-year in static and rotating states, respectively.

One measure which helps to determine the electrical-power-plant capacity factor is the plant factor. This compares the amount of power-plant generated electricity to its maximum potential generation capacity over a specific period of time [27].

The yearly maximum-potential-generation capacity of solar panels can be determined by multiplying its nominal power by the used number of hours per year, assuming it works over 24 hours per day. In this case, it will be assumed to be 24 hours per day even if it is not physically possible because the sun does not appear during the day and night. However, this is often used in the design and evaluation of photovoltaic solar energy systems. So, the equation for the plant factor is the one in (2), where p_f is the plant factor, G_E is the generated

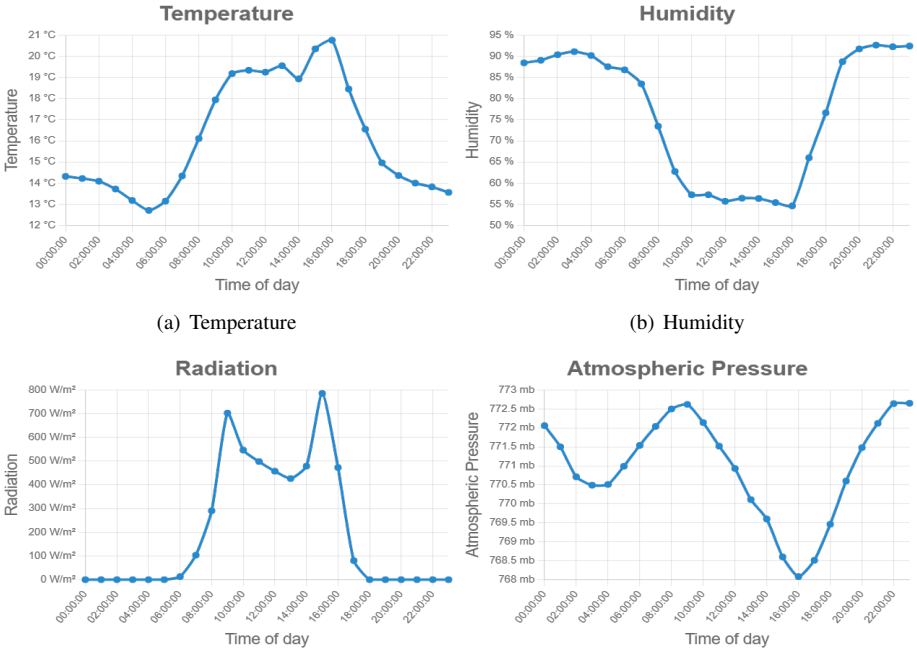

(a) Temperature (b) Humidity

(c) Radiation (d) Atmospheric pressure

Figure 9. Examples of weather graphs shown in the webpage.

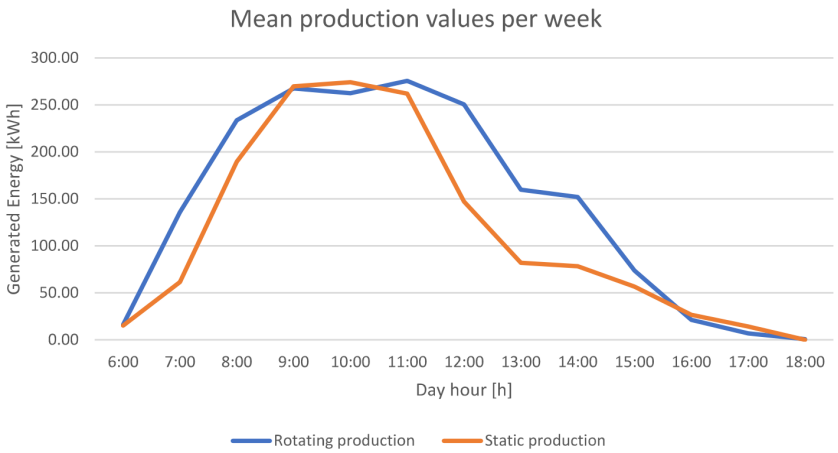

Figure 10. Weekly graph production.

energy, N_P is the solar panel nominal power, and 8.76 results from the multiplication of 24 hours per day by 365 days per year and divided by 1000 to get the corresponding value in kWh-year.

$$p_f = \frac{G_E}{N_P \times 8.76} \tag{2}$$

Notice that for a 250-W solar panel, the denominator of (2) will be the following:

$$250\,\mathrm{W} \times 8.76\,\mathrm{kh} - \mathrm{year} = 2190\,\mathrm{kWh} - \mathrm{year}$$

So, performing the ratio in (2) for the previous generations, the static-state plant factor is 22.65 % and the rotating-state one is 29.25 %. As can be seen, there is a 6.60-point difference between both factors, indicating that the rotating system generates more than when it is static. Regarding energy production, the final difference is about 144.56 kWh-year.

On the other hand, it is possible to get the solar-equivalent hours from these measures and compare it with the 4.94 solar hours registered in Quito for November according to CONELEC (2024). Static production would be used for this analysis because it could be considered a normal measurement. Equation (3) shows how to get those hours per day, where s_h are the solar hours, G_E is the generated energy, N_P is the solar panel nominal power and 365 because it is the number of days over a day.

$$s_h = \frac{G_E}{N_P \times 365} \tag{3}$$

For a 495.94 kWh-year generation with a 250-W solar panel, there are 5.44 solar equivalent hours. There are only 0.5-hours difference between the value shown in CONELEC (2024) and the calculated one, so it is possible to say that they are equivalent.

4 Discussion

In the Section , it is observed that the tracking system enhances solar panel energy production. However, the validity of these results depends on consistent testing conditions throughout the year. It assessed the project's cost-effectiveness through cash flow analysis, which involves two key metrics: net present value (NPV) and internal rate of return (IRR). NPV measures the investment's profitability by comparing the present value of expected cash flows with the initial investment cost. A positive NPV signifies a financially appealing investment, while a negative NPV suggests otherwise. IRR, on the other hand, represents the discount rate that renders the NPV zero. A positive IRR indicates a positive return, while a negative IRR suggests a negative return [29].

For this project, the lifetime of the project must be established. A solar panel can work well for 25 years, so this value will be taken as reference for the analysis. Also, the cost of the prototype, without considering the monitor, neither the batteries nor other extra components, must be taken, being $ 200. With a yearly solar panel depreciation of 0.5%, the final results from the cash flow analysis can be observed in Table 2. It can be seen that the project is not viable in Ecuador with a subsidized price, as both the NPV and IRR are negative, indicating significant losses. However, if the price is unsubsidized, the project becomes profitable and may be of interest to public power-generating companies such as CENACE. Alternatively, if the project is implemented in countries like Spain or Brazil, it will be highly profitable due to the higher electricity prices in those regions.

It is worth noting that this prototype utilizes a single solar panel, but scalability is possible. For example, expanding to three solar panels increases generation to 433.68 kWh, resulting in

Table 2. Cash flow analysis for different scenarios

Scenario	Electricity tariff [USD/kWh]	NPV [USD]	IRR [%]
Ecuador (subsidized)	0.092	-96.51	-2.51
Ecuador (unsubsidized)	0.142	48.20	3.95
Brasil	0.19	141.10	8.95
Spain	0.33	413.21	21.14

a profitable NPV of 39.22 USD and an IRR of 8.36% in the subsidized case in Ecuador, albeit at increased cost. Additionally, supporting higher capacity panels, such as 1 kW, promises increased production and profitability. Comparing results with other studies conducted in Ecuador, the project's performance stands out. A study in Milagro, Ecuador, reported a modest increase of 59.74 kWh in energy generation. This disparity may be attributed to the use of smaller solar panels, although specifics are not provided in the study.

Production comparisons between months, with and without a solar tracker, conducted in Quito, resulted in a 21.3 kWh monthly increase, equivalent to 255.6 kWh annually, utilizing a mono-crystalline 330-W solar panel [20].

In contrast, a single-axis tracking system in Quito achieved a plant factor of 27.3%, closely resembling the 29.25% attained in this study. However, as these results were obtained via simulation, direct panel comparison is unfeasible [30].

Comparatively, the static system yields 1459 kWh daily, while the rotating system produces 1856 kWh. Though insufficient for a 2500 kWh residence, the rotating system approaches the target, highlighting its potential scalability and profitability with larger panels and increased scale.

5 Conclusions

The single-axis solar tracker made up a gear-worm mechanism for the rotation attached to a motor controlled by artificial intelligence fulfils its function, generating 144.56 kWh-year with a power plant of 29.25 %. Even though it is a great value, it could be improved if the system is adapted to support bigger and more powerful solar panels, generating 433.68 kWh, red(NPV: 39.22 USD, IRR: 8.36%), enhancing the production. Additionally, even if its profitability is not so exploited in Ecuador due to its geographical location, this prototype could be functional in other countries, such as redSpain (NPV: 413.21 USD, IRR: 21.14%) or Brazil (NPV: 141.10 USD, IRR: 8.95%).

On the other hand, the environmental measures were enough to predict the correct tilt angle so that the solar panel could catch the higher number of perpendicular radiation rays. Moreover, the rotating mechanism supported the 50 MPa generated by the solar panel, preventing any instability issues during the implementation. redIt must be noted the motor capable to manage this only 0.072 Wh, less than the 0.01 % of the total production. Furthermore, the virtual web monitor works to accomplish its purpose of showing the project measures during its lifetime and internally saving the information with a token security method.

References

1. Agencia de Regulación y Control de Energía y Recursos Naturales no Renovables, *Balance Nacional de Energía Eléctrica. Ministerio de Energía y Minas,* (Quito, Ecuador, 2023) https://www.controlrecursosyenergia.gob.ec/balance-nacional-de-energia-electrica/. Last accessed 10 March 2024.

2. P. Dechamps, *The IEA World Energy Outlook 2022 – a brief analysis and implications,* The European Energy and Climate Journal, 11(3), 100-103 (2023) https://doi.org/10.4337/eecj.2023.03.05
3. Q.Hassan, P.Viktor, T. J. Al-Musawi, B. Mahmood Ali, S. Algburi, H. M. Alzoubi, A. K. Al-Jiboory, A. Sameen, M. Hayder, M. Jaszczur, *The renewable energy role in the global energy transformation. Renewable Energy Focus,* **48**, 100545 (2024).
4. Y. Nassar, M. Khaleel, *Sustainable Development and the Surge in Electricity Demand Across Emerging Economies,* Int. J. Electr. Eng. and Sustain. **2**(1), 51-60 (2024).
5. M. Büchs, N. Cass, C. Mullen, K. Lucas, D. Ivanova, *Emissions savings from equitable energy demand reduction,* Nature Energy **8**(7), 758-769 (2023).
6. P. A. Østergaard, N. Duic, Y. Noorollahi, H. Mikulcic, S. Kalogirou, *Sustainable development using renewable energy technology,* Renewable energy **146**, 2430-2437 (2020).
7. J. Cevallos-Sierra, J. Ramos-Martin, *Spatial assessment of the potential of renewable energy: The case of Ecuador,* Renewable and Sustainable Energy Reviews **81**, 1154-1165 (2018).
8. M. E. Z. Zapata, E. C. P. Carpio, A. R. C. Alava, J. O. Y. Márquez, M. E. M. Soto, V. J. G. Montealegre, *Economic feasibility study on a banana farm applying alternative energy: photovoltaic,* South Florida Journal of Development **3**(4), 5159-5172 (2022).
9. X. Zhikun, *Research and design of control system of the solar panel tracking,* 2016 IEEE Advanced Information Management, Communicates, Electronic and Automation Control Conference (IMCEC), Xi'an, China, pp. 1384-1388 (2016).
10. M. A. Ponce-Jara, C. Velásquez-Figueroa, M. Reyes-Mero, C. Rus-Casas, *Performance Comparison between Fixed and Dual-Axis Sun-Tracking Photovoltaic Panels with an IoT Monitoring System in the Coastal Region of Ecuador,* Sustainability **14**(3), 1696 (2022).
11. M. M. Reyes, S. Tuárez, I. Fernando, *Análisis Comparativo Técnico-Económico Entre Paneles Solares Estáticos y Paneles Con Sistema De Seguimiento De Dos Ejes Instalados En La Ciudad De Manta-ULEAM, Undergraduare thesis,* Facultad de Ingeniería, Universidad Laica Eloy Alfaro de Manabí (2021).
12. D. D. Fiallos Chamorro, *Determinación del punto óptimo de potencia de paneles fotovoltaicos en base a variables difusas mediante el modelo de Liu Jordan, Undergraduare thesis,* Ingeniería Eléctrica, Universidad Politécnica Salesiana (2020).
13. S. V. Arpi Puga, B. G. Prado Bermeo. *Diseño de un seguidor solar de doble eje para un sistema de energía fotovoltaica en el centro de salud de la comunidad de Yaapi, Undergraduare thesis,* Ingeniería Mecatrónica, Universidad Politécnica Salesiana (2022).
14. F. I. Mustafa, S. Shakir, F. F. Mustafa, A. T. Naiyf. *Simple design and implementation of solar tracking system two axis with four sensors for Baghdad city,* In 2018 9th International Renewable Energy Congress (IREC), pp. 1-5. IEEE, Hammamet, Tunisia (2018).
15. M. Singh, J. Singh, A. Garg, E. Sidhu, V. Singh, A. Nag, *Efficient autonomous solar energy harvesting system utilizing dynamic offset feed mirrored parabolic dish integrated solar panel*, In 2016 International Conference on Wireless Communications, Signal Processing and Networking (WiSPNET), pp. 1825-1829, IEEE, Chennai, India (2016).
16. D. A. Mejía, I. T. Chávez, A. Mejía, *Positioning control of square arrangements of solar panels by solar tracing using fuzzy logic,* South Florida Journal of Development **2**(2), 3318-3331 (2021).
17. M. A. Alarcón, R. G. Alarcón, A. H. González, A. Ferramosca, *Modeling a residential microgrid for energy management,* In 2020 Argentine Conference on Automatic Control (AADECA), pp. 1-6, IEEE, Buenos Aires, Argentina (2020).

18. S. K. Sahoo, M. Balamurugan, S. Anurag, R. Kumar, V. Priya, *Maximum power point tracking for PV panels using ant colony optimization,* In 2017 Innovations in Power and Advanced Computing Technologies (i-PACT), pp. 1-4, IEEE, Vellore, India, (2017).
19. M. R. Haider, A. Shufian, M. N. Alam, M. I. Hossain, R. Islam, M. A. Azim, *Design and implementation of three-axis solar tracking system with high efficiency,* In 2021 International Conference on Information and Communication Technology for Sustainable Development (ICICT4SD), pp. 1-5, IEEE, Dhaka, Bangladesh (2021).
20. J. F. Agila Díaz, L. A. Landázuri Ayala, *Diseño y construcción de un sistema de rastreo solar biaxial para generación de 600 Wh de energía eléctrica, Undergraduare thesis,* Ingeniería Mecánica, Universidad Politécnica Salesiana (2021).
21. FireBeetle ESP32 IoT Microcontroller (Supports Wi-Fi and Bluetooth), https://www.dfrobot.com/product-1590.htm. Last accessed 13 March 2024
22. Secretaría de Ambiente del Municipio del Distrito Metropolitano Quito, *Datos historicos remmaq,* (2022). http://www.quitoambiente.gob.ec/index.php/descarga-datos-historico. Last accessed 27 March 2023
23. *Calculation of sun position in the sky for each location on the earth at any time of day. Azimuth, sunrise sunset noon, daylight, and graphs of the solar path,* https://www.sunearthtools.com/dp/tools/pos_sun.php. Last accessed 13 March 2024
24. J. S. Fuentevilla, M. Ávalos, D. García, *Diseño y construcción de un sistema de seguimiento fotovoltaico,* Universidad Tecnológica de la Mixteca, 2012.
25. W. X. García-Quilachamin, J. E. Sanchez-Cano, J. Herrera-Tapia, E. J. Velesaca-Zambrano, *Analysis of A Two-Axis Solar Tracker System: Case Study,* International Journal of Online and Biomedical Engineering (iJOE), 17(05), pp. 147–164 (2021).
26. H. A. E.-m. Salama, A. T. M. Taha, *Practical Implementation of Dual Axis Solar Power Tracking System,* In 2018 Twentieth International Middle East Power Systems Conference (MEPCON), pp. 446-451, IEEE, Cairo, Egypt (2018).
27. M. Boxwell, *The Solar Electricity Handbook-2017 Edition: A simple, practical guide to solar energy–designing and installing solar photovoltaic systems,* Greenstream Publishing (2017).
28. CONELEC. *Atlas Solar del Ecuador con fines de generación eléctrica.* https://biblioteca.olade.org/opac-tmpl/Documentos/cg00041.pdf. Last accessed 13 March 2024
29. E. F. Brigham, *Financial management: Theory and practice. Cengage Learning Canada Inc* (2016).
30. F. Ordóñez, C. Morales, J. López-Villada, S. Vaca, *Assessment of the energy gain of photovoltaic systems by using solar tracking in equatorial regions,* Journal of Solar Energy Engineering **140**(3), 031003 (2018).